Original Article

A novel *ODAPH* mutation causing amelogenesis imperfecta and its expression in human dental tissues

Shih-Kai Wang [a,b]*, Zhe-Hao Lee [a], Parissa Aref [c], Kuan-Yu Chu [b]

[a] Department of Dentistry, National Taiwan University School of Dentistry, Taipei, Taiwan
[b] Department of Pediatric Dentistry, National Taiwan University Children's Hospital, Taipei, Taiwan
[c] Department of Pediatric Dentistry, Islamic Azad University Dental Branch of Tehran, Tehran, Iran

Abstract *Background/purpose:* Amelogenesis imperfecta (AI), an assemblage of genetic diseases with dental enamel malformations, is generally grouped into hypoplastic, hypomaturation, and hypocalcified types. This study aimed to identify the genetic etiology for a consanguineous Iranian family with autosomal recessive hypocalcified AI.

Materials and methods: Dental defects were characterized, and whole exome analysis conducted to search for disease-causing mutations. Minigene assay and RT-PCR were performed to evaluate molecular consequences of the identified mutation and expression of the causative gene in human dental tissues.

Results: The defective enamel of erupted teeth showed extensive post-eruptive failure and discoloration. Partial enamel hypoplasia and indistinct dentino-enamel junction were evident on unerupted teeth, resembling hypocalcified AI. A novel homozygous *ODAPH* (previously designated *C4orf26*) mutation of single-nucleotide deletion (NG_032974.1:g.5103del, NM_178497.5:c.67+1del) was identified to be disease-causing. The mutation would cause a frameshift to different *ODAPH* transcript variant (TV) products: p.(Ala23Hisfs*29) for TV1 and p.(Gly23Aspfs*140) for TV2. Both dental pulps of developing and exfoliating primary teeth expressed *ODAPH* TV2.

Conclusion: Loss-of-function *ODAPH* mutations can cause AI type IIIB (the hypocalcified, autosomal recessive type), rather than type IIA4 (the hypomaturation, pigmented autosomal recessive type). This study supports a hypothesis that the product of *ODAPH* TV2 is the single dominant ODAPH protein isoform critical for dental enamel formation and may also play an unappreciated role in development and homeostasis of dentin-pulp complex. Due to genetic heterogeneity and a nonideal genotype-phenotype correlation of AI, it is essential to perform genetic testing for patients with inherited enamel defects to make a definitive diagnosis.

* Corresponding author. Department of Dentistry, National Taiwan University School of Dentistry, No. 1, Changde St., Zhongzheng Dist., Taipei 100229, Taiwan.
E-mail address: shihkaiw@ntu.edu.tw (S.-K. Wang).

Introduction

Amelogenesis imperfecta (AI) is a categorical diagnosis for inherited disorders characterized by malformation of dental enamel with or without non-dental abnormalities.[1,2] Currently, Witkop's classification is the most commonly used classification system for AI. Based upon clinical characteristics of the enamel defects and mode of disease inheritance, AI is grouped into 4 main types: hypoplastic (type I), hypomaturation (type II), hypocalcified (type III), and hypomaturation-hypoplastic with taurodontism (type IV).[2] While enamel with a reduced thickness is described as hypoplastic AI, that with a hardness defect is termed hypomaturation. Hypocalcified AI, on the other hand, delineates malformed enamel consisting of poorly calcified matrix and prone to discoloration and post-eruptive failure. Extensive genetic research has identified at least 15 causative genes responsible for non-syndromic AI of various types,[3] such as *AMELX*,[4] *ENAM*,[5] *AMBN*,[6] *MMP20*,[7] *KLK4*,[8] *FAM83H*,[9] *WDR72*,[10] *ODAPH*,[11] *SLC24A4*,[12] *ITGB6*,[13,14] *GPR68*,[15] *ACP4*,[16] *RELT*,[17] *DLX3*,[18] and *LAMB3*.[19,20] Genetic heterogeneity and overlapping genotype-phenotype correlations make it impractical to reach a definitive diagnosis for AI clinically and render the necessity of genetic testing.

Odontogenesis-Associated Phosphoprotein (*ODAPH*, OMIM ∗614829) was designated Chromosome 4 Open Reading Frame 26 (*C4orf26*) when it was first discovered to cause autosomal recessive AI.[11] *ODAPH* localizes to chromosome 4q21.1 between the dentin/bone and glutamine/proline groups of secretory calcium-binding phosphoprotein (SCPP) genes, although *ODAPH* itself is not an SCPP gene.[21] It contains 3 exons and is predicted to encode secreted proteins with 3 distinct isoforms originated from 3 alternatively spliced *ODAPH* transcripts. Transcript variant 1 (TV1, NM_001206981.2) includes all exons and represents the longest transcript, which encodes a protein precursor of 176 amino acids (isoform 1). Both transcript variants 2 and 3 (TV2, NM_178497.5; TV3, NM_001257072.2) skip exon 2, which causes a frameshift and hits an earlier translation termination codon in exon 3 compared to TV1. TV3 has the same reading frame as that of TV2 and is distinguished from TV2 by the removal of an internal exon 3 segment (135 bps) through alternative splicing. They encode protein precursors of 130 (isoform 2) and 85 (isoform 3) amino acids respectively. All 3 ODAPH isoforms are predicted to have a 23-amino-acid signal peptide, which is encoded almost exclusively by exon 1.[11,21]

In this study, we characterized a family of autosomal recessive AI and identified a novel *ODAPH* disease-causing mutation. The results gain a better insight into the enamel phenotypes of *ODAPH*-associated AI and argue for ODAPH isoform 2 playing an essential role in dental enamel formation. We also demonstrated differential expression of *ODAPH* in various tissues of human teeth, suggesting it has potential functions during tooth development other than enamel formation.

Materials and methods

Enrollment of human subjects

The study was reviewed and approved by the Institutional Review Boards at the Islamic Azad University and the National Taiwan University Hospital. In compliance with the Declaration of Helsinki, subject enrollment, clinical examinations, and collection of saliva samples were performed with the understanding and written consent of each participant. Clinical physical examinations and dental radiographs were conducted to characterize disease phenotypes and history taking to construct the family pedigree.

Mutational analyses

Non-stimulated saliva (2 mL) from each research subject was collected to obtain the genomic DNA. For the proband of the family, whole exome sequencing and bioinformatic analyses were conducted as previously described in search of disease-causing mutations.[22] Following identification of the *ODAPH* mutation, Sanger sequencing was further performed for confirmation. The *ODAPH* Exon 1 and its flanking sequences were amplified as a 439-bp product using 5′-GTTGTCCAAAATCCCCCT-3′ (forward) and 5′-TAACCACA-CAGGCTGATG-3′ (reverse) primers. For sequence variant calling and annotation, human reference sequence NG_032974.1, NM_001206981.2, NM_178497.5, and NM_001257072.2 were employed for numbering gDNA and cDNA (TV1, TV2, and TV3) positions respectively. All sequence variation designations were verified using LUMC Mutalyzer 2.0.32.[23]

Minigene splicing assay

A 1621-bp genomic DNA fragment of human *ODAPH* was amplified and subcloned into the pcDNA3.1(+) vector to generate an *ODAPH* minigene construct. The fragment spanned from the 5′ upstream region of *ODAPH* to its termination codon on Exon 3 (NG_032974.1:g.4984_13486) but excluded part of Intron 2 (NG_032974.1:g.5852_12733). The mutant construct of the *ODAPH* splice-site mutation identified in our family (NG_032974.1:g.5103del; NM_178497.5:c.67+1del) was then generated through site-directed mutagenesis. HEK293T and COS-7 cells, cultured in 6-well plates, were transfected with 2.5 μg of wild-type or mutant minigene plasmids. After 24h, the cells were harvested, and total RNA extracted, converted to cDNA, and amplified using *ODAPH*-specific primers (5′-TGGTATGCT GGTTGGTGGTA-3′ and 5′-CCCTCTCAGCTTTCCTCAGA-3′).

The amplified products were separated by agarose gel electrophoresis and analyzed by Sanger sequencing.

Tissue preparation and reverse transcription polymerase chain reaction

Five different tissues from human teeth were analyzed for gene expression. Dental pulps were harvested from an exfoliated primary mandibular second molar and an extracted natal tooth. Dental follicles, periodontal ligaments, and apical papillae of developing teeth were obtained from an extracted supernumerary tooth (mesiodens). Total RNA was extracted from each tissue. Gene expression was analyzed by PCR amplification using cDNA, reverse transcribed from 0.1 μg of total RNA, with specific primers for *ODAPH*, *DSPP* (dentin sialophosphoprotein, NM_014208.3), *KLK4* (kallikrein related peptidase 4, NM_004917.5), *AMTN* (amelotin, NM_212557.4), and *GAPDH* (glyceraldehyde-3-phosphate dehydrogenase, NM_002046.7) (Table S1).

Results

A novel *ODAPH* disease-causing mutation

We identified a consanguineous Iranian family with hypocalcified amelogenesis imperfecta presenting in the youngest generation (Fig. 1). The proband (IV:2) was a 27-year-old male born to a first-cousin marriage. Clinically, he had multiple absent teeth and a severe anterior open-bite. The missing teeth were previously extracted due to unrestorable defects. The remaining teeth exhibited severe attrition and heavy brown-black discoloration. Exposure of dentin was evident in many teeth, causing hypersensitivity to thermal stimulation and difficulty maintaining oral hygiene. The panoramic radiograph revealed that teeth #6, 7, 8, 9, 10, 11, 22, and 27 had failed to erupt (Fig. 1a). There was no distinct dentino-enamel junction (DEJ) of these unerupted teeth radiographically, indicating a hypomineralization enamel defect. Noticeably, the enamel layer of the impacted teeth, such as tooth #27, was not of a full thickness, suggesting a concomitant hypoplastic defect. In contrast, the dentin appeared normal, although multiple carious lesions were present. While his parents and older brother (IV:1) were not affected, his younger brother (IV:3) and sister (IV:4) had similar dental phenotypes, suggesting an autosomal recessive manner of disease inheritance (Fig. 1b).

Whole-exome analyses of proband's DNA identified 92 homozygous mutations predicted to be "probably damaging" by PolyPhen-2[24] after filtering out sequence variants with a MAF (minor allele frequency) of 1% or more in dbSNP (153), NHLBI-ESP, or gnomAD databases (Table S2). A single nucleotide deletion (NG_032974.1:g.5103del) in *ODAPH* was the only deleterious mutation identified in a known AI candidate gene (Fig. 1c). In the human *ODAPH* gene, translation initiates in exon 1. The last nucleotide of exon 1 and the first nucleotide of intron 1 are both Gs. In this patient, one of these two Gs was deleted. The Human Genome Variation Society's (HGVS) established standards for nomenclature requires that this deletion be described as the loss of the second G (in the intron): NM_178497.5:c.67+1del, rather than NM_178497.5:c.67del.

Aberrant RNA splicing caused by the mutation

To investigate how this single nucleotide deletion at the exon 1/intron 1 junction (NM_178497.5:c.67+1del) affects normal splicing of *ODAPH*, we conducted a minigene assay using HEK293T and COS-7 cells (Fig. 2a). Under transfection of the wild-type construct, a 364-bp product of *ODAPH* TV2 was amplified from both cells, while a 408-bp amplicon from *ODAPH* TV1 was only detected in COS-7. However, when transfected with the mutant minigene, both cells exhibited 3 major amplification products of different sizes. The 2 smaller products of 363 and 407 bps were identical to those from the wild-type minigene but one-nucleotide shorter due to the G deletion. The largest product was a 798-bp amplicon resulting from inclusion of intron 1 (391 bps) to mutant *ODAPH* TV1 (407 bps). These 3 mutant transcripts were all expected to be nonfunctional. The mutant TV1 and TV2 with a −1 frameshift would produce a truncated ODAPH isoform 1, p.(Ala23Hisfs*29), and an abnormal isoform 2, p.(Gly23Aspfs*140). On the other hand, the mutant TV1 with intron 1 retention would presumably undergo nonsense mediated decay due to an early premature termination codon or generated an aberrant ODAPH protein, p.(Gly23Valfs*14). In other words, whether the intron is removed by RNA splicing (causing a −1 frameshift) or retained (translating through the intron), only the first 22 amino acids of the signal peptide would be synthesized correctly, and none of the secreted protein itself. Therefore, the enamel in this proband formed in the absence of ODAPH protein, with little possibility that the phenotype could have been made more severe by expression of a mutated protein (see discussion).

ODAPH expression in dental pulps

To evaluate expression of *ODAPH* and related genes involved in biomineralization in human teeth, we performed RT-PCR for 5 tissues: dental pulps from shedding (SPu) and developing (NPu) primary teeth, dental follicles (Flc), periodontal ligaments (PDL), and apical papillae (AP) (Fig. 2b). While PDL and AP cells did not show measurable *ODAPH* expression, a 364-bp amplicon was highly detected in dental pulp cells, both SPu and NPu, and slightly from dental follicle cells, indicating an expression of *ODAPH* TV2. Neither TV1 (408 bps) nor TV3 (229 bps) was observed in any analyzed tissues. *DSPP* expression was strongly detected in NPu, but not SPu, cells, indicating active dentin formation in developing primary teeth. AP cells and PDL also showed moderate and weak *DSPP* expressions respectively. On the other hand, only tissues from dental follicles exhibited detectable expression of *KLK4*, a marker for maturation stage ameloblasts. In contrast, *AMTN*, another maturation stage gene, was observed in all tissues except for AP cells.

Discussion

Currently, OMIM (Online Mendelian Inheritance in Man) database designates *ODAPH*-associated enamel defects as
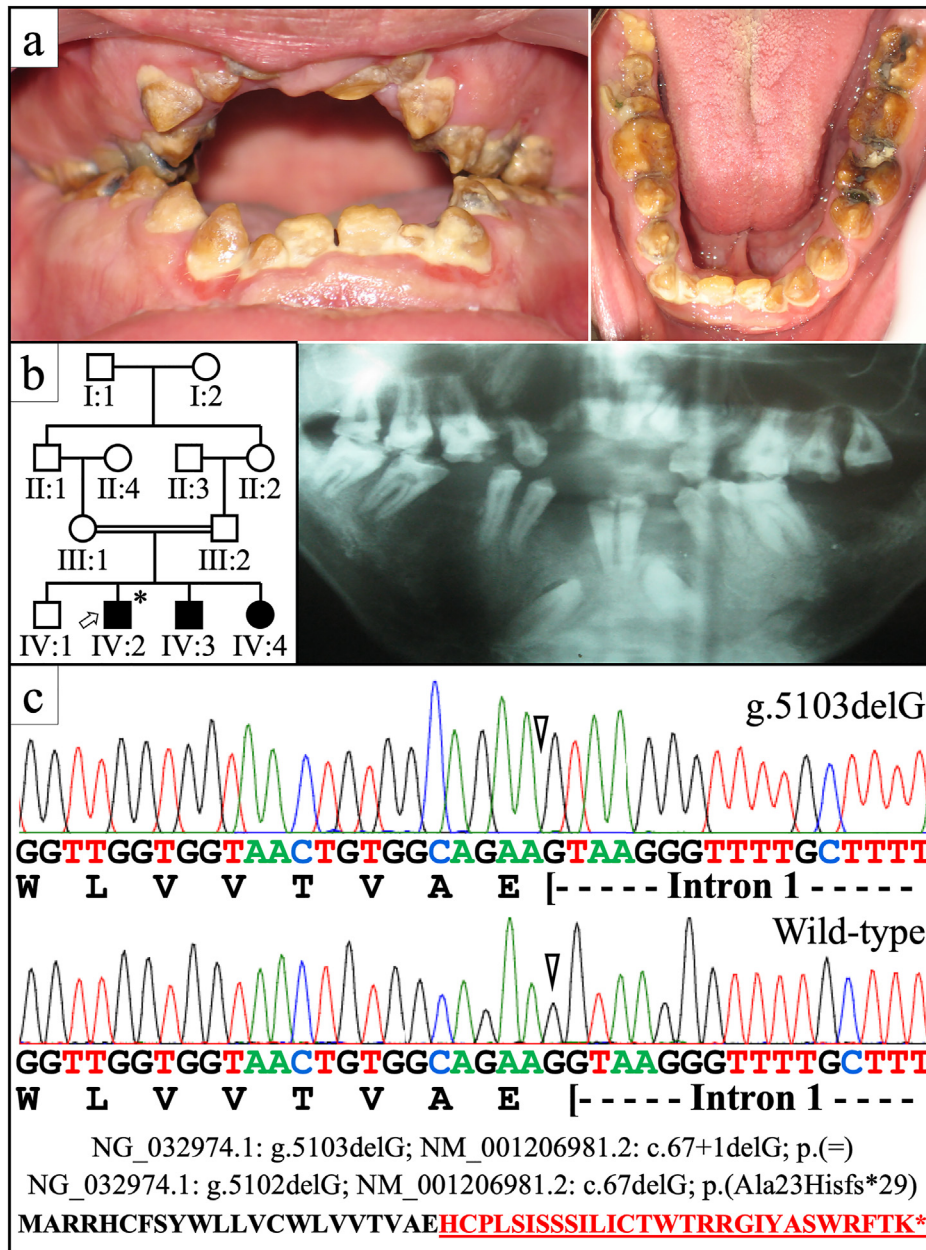
Figure 1 **The AI family with a novel *ODAPH* mutation.** **(a)** The proband's (IV:2) panorex shows multiple impacted teeth, which exhibit partial enamel hypoplasia and no contrast between enamel and dentin. Clinical photos of proband's affected brother (IV:3) reveal severe post-eruptive enamel failure and brown-black discoloration of all permanent teeth. **(b)** The family pedigree demonstrates 3 affected individuals from a consanguineous marriage and suggests a recessive pattern of inheritance. **(c)** The DNA sequencing chromatogram shows a G deletion from the reference sequence that would cause a −1 frameshift in both *ODAPH* allele. The resulting mutant protein is predicted based on *ODAPH* transcript variant 1 (NM_001206981.2). AI, amelogenesis imperfecta.

AI type IIA4, a subtype of hypomaturation AI. According to Witkop's classification, AI type IIA (the hypomaturation, pigmented autosomal recessive type) has enamel that shows a clear to cloudy, mottled, agar-brown color but of normal thickness.[1,2] The enamel is softer than normal and fractures from dentin. In addition to *ODAPH*, hypomaturation AIs caused by *KLK4*, *MMP20*, *WDR72*, *SLC24A4*, and *GPR68* mutations have been categorized under this subtype as types IIA1, IIA2, IIA3, IIA5, and IIA6 respectively.[7,8,10,12,15] However, unlike the enamel phenotype caused by

mutations in these other genes, the affected enamel in our proband exhibits a reduced thickness to some extent on unerupted teeth. Many erupted teeth show extensive enamel chipping and attrition leaving exposed dentin, which highly resembles the defects of hypocalcified AI.[1,2] Reviewing available clinical data from the previous 2 reports of *ODAPH* mutations,[11,25] we also found the enamel phenotypes of documented families are similar to hypocalcified rather than hypomaturation AI. Therefore, we argue that *ODAPH*-associated enamel defects should be
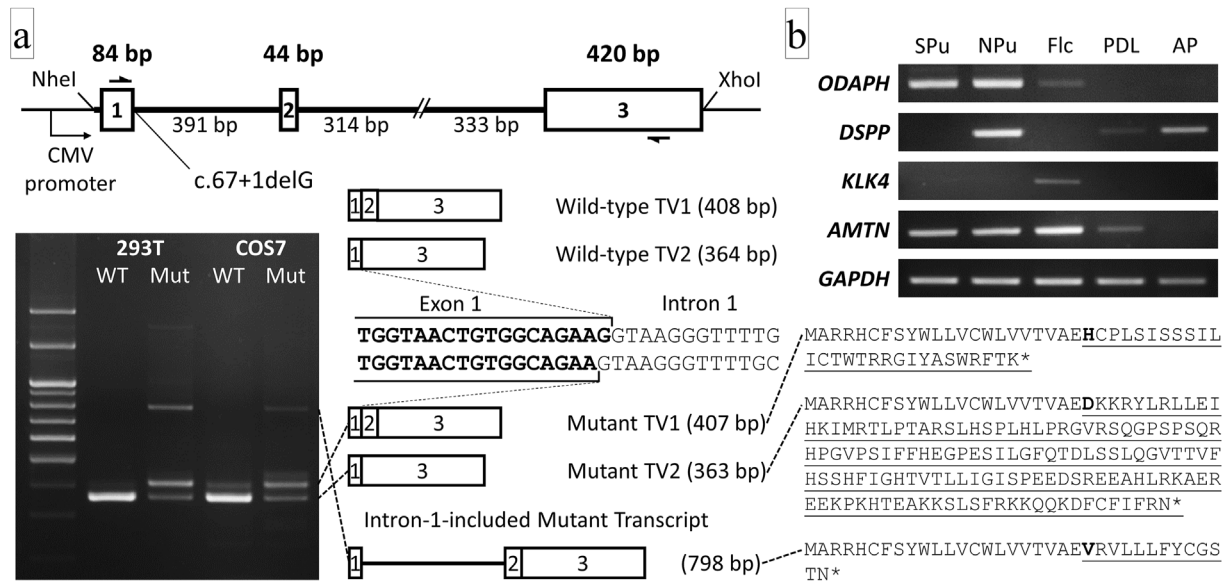
Figure 2 Altered mRNA splicing caused by the *ODAPH* mutation and *ODAPH* expression in human dental tissues. (a) The minigene assay shows 3 main mutant transcripts resulting from the c.67+1del mutation: G-deleted TV1, G-deleted TV2, and G-deleted TV1 with Intron 1 retention. The hypothetical proteins generated from each mutant transcript respectively are presented at the lower right corner of the figure. (b) RT-PCRs demonstrate that *ODAPH* TV2, but not TV1 or TV3, is strongly expressed by pulp tissues of primary teeth and slightly in dental follicles of erupting teeth. No expression is detected from PDL or apical papilla tissues. mRNA, messenger RNA; TV, transcript variant; RT-PCR, reverse transcription polymerase chain reaction; SPu, dental pulp of a shedding primary tooth; NPu, dental pulp of a natal tooth; Flc, dental follicle; PDL, periodontal ligament; AP, apical papilla.

categorized as AI type IIIB (the hypocalcified, autosomal recessive type) instead of AI type IIA4.

To date, 7 different *ODAPH* mutations have been reported to be disease-causing, including 3 insertion-deletion (indel) and 4 point mutations (Table 1).[11,25] As transcript variant 1 (TV1) of human *ODAPH* encodes a different translation reading frame from that of transcript variants 2 and 3, the disease-causing mutations have distinct impacts on products of these transcripts (Fig. 3). The most 5′

mutation is an 8-nucleotide deletion in exon 1, and the second one a 6-nucleotide deletion replaced by 16 others (a net gain of 10 nucleotides). Both mutations cause a −2 frameshift and introduce a premature termination codon in exon 3 (the second exon of TV2). While the mutant transcripts would presumably escape nonsense mediated decay, the resulting proteins have neither the normal C-terminus nor the intact signal peptide of wild-type ODAPHs and would probably not be secreted, indicating a complete loss

Table 1 Seven known *ODAPH* AI-causing mutations.

#	Gene (NG_032974.1)	TV1 (NM_001206981.2) TV2 (NM_178497.5)	Protein	Refs
1	g.5074_5081del	**TV1:** c.39_46del	p.(Cys14Glyfs*18)	[25]
	g.5074_5081del	**TV2:** c.39_46del	p.(Cys14Glyfs*21)	
2	g.5086_5091delinsATGCTGGTTACTGGTA	**TV1:** c.51_56delinsATGCTGGTTACTGGTA	p.(Val18Cysfs*20)	[11]
	g.5086_5091delinsATGCTGGTTACTGGTA	**TV2:** c.51_56delinsATGCTGGTTACTGGTA	p.(Val18Cysfs*23)	
3	g.5103del	**TV1:** c.67+1del	p.(Ala23Hisfs*29)	this
	g.5103del	**TV2:** c.67+1del	p.(Gly23Aspfs*140)	study
4	g.13065A > T	**TV1:** c.112-2A > T	p.(?)	[11]
	g.13065A > T	**TV2:** c.68-2A > T	p.(?)	
5	g.13128C > A	**TV1:** c.173C > A	p.(Ala58Asp)	[11]
	g.13128C > A	**TV2:** c.129C > A	p.(Cys43*)	
6	g.13228C > T	**TV1:** c.273C > T	p.(=)	[11]
	g.13228C > T	**TV2:** c.229C > T	p.(Arg77*)	
7	g.13317G > A	**TV1:** c.362G > A	p.(Gly121Asp)	[11]
	g.13317G > A	**TV2:** c.318G > A	p.(Trp106*)	

Genomic mutation designations start from the beginning of the *ODAPH* gene reference (NG_032974.1), which has the ATG translation initiation codon in exon 1 starting at nucleotide 5036. The cDNA designations correspond to the TV1 (NM_001206981.2) and TV2 (NM_178497.5) references, with the A of the ATG translation initiation codon assigned as nucleotide 1. (See notes at Supplementary Material) AI, amelogenesis imperfecta; TV, transcript variant.
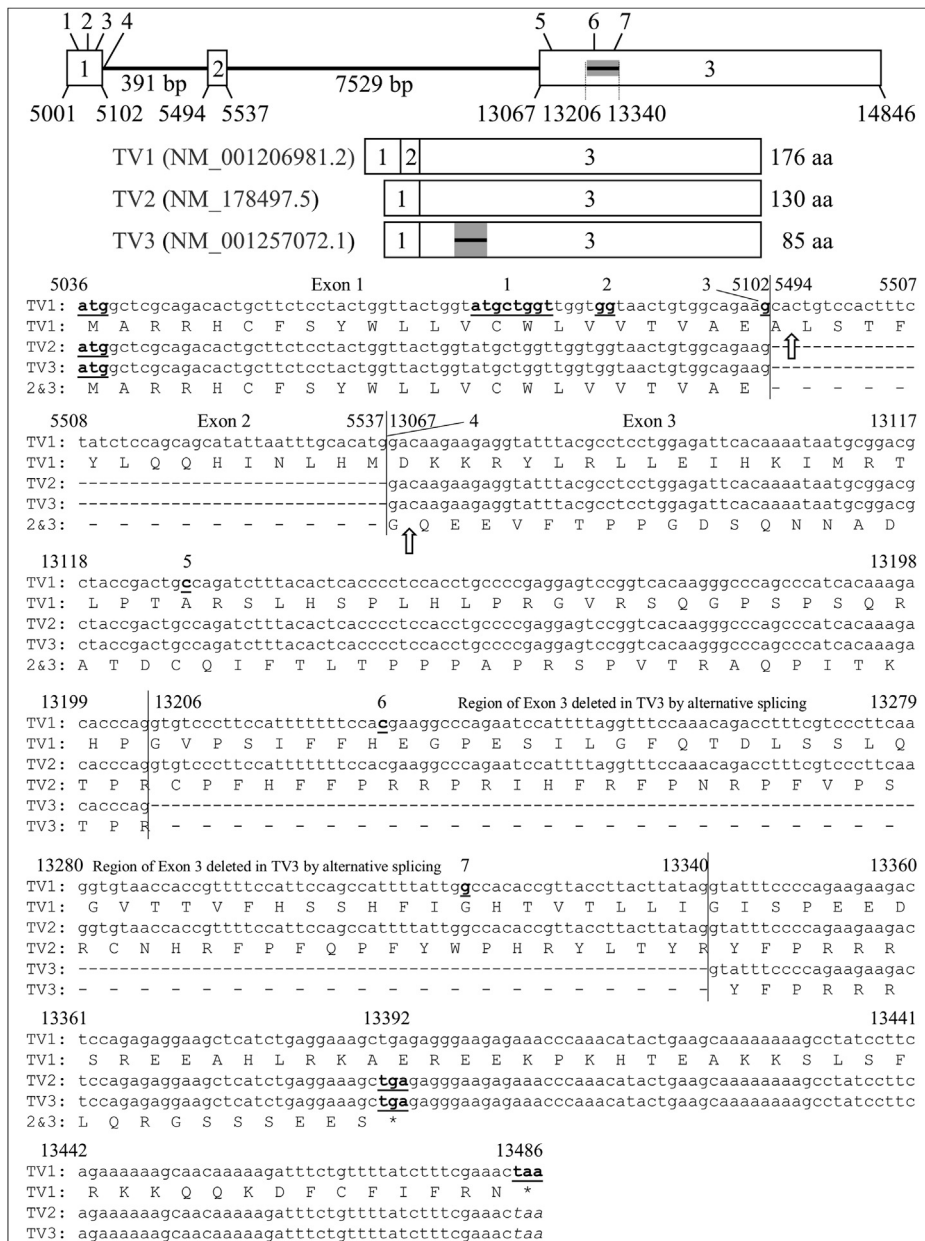
Figure 3 *ODAPH* transcript variants, coding regions, and AI-causing mutations. *ODAPH* gene structure at the top shows 3 coding exons and the locations of the 7 known AI-causing mutations. Numbers at the bottom of the gene diagram correspond to the *ODAPH* gene reference sequence NG_032974.1. Alignment of the coding sequences of TV1, TV2, and TV3. Translation initiation and termination codons and AI mutation sites are in bold and underlined. Note that exon 2 shifts the reading frame of TV1 relative to TV2 and TV3. Upward arrows mark the signal peptide cleavage site. Note that only TV1 includes exon 2, which shifts the reading frame of exon 3 relative to TV2 and TV3. TV3 is distinguished from TV2 by the removal of an internal exon 3 segment through alternative splicing (13206—13340). (See notes at Supplementary Material) AI, amelogenesis imperfecta; TV, transcript variant.

of function of all ODAPH isoforms or a potential cell pathology caused by intracellular accumulation of aberrant proteins. The third mutation is a single nucleotide deletion identified in this study. Although HGVS nomenclature requires that this deletion be described as the loss of the second G (at intron 1), there is still a GT that would likely support normal splicing, but result in the loss of a G at the end of exon 1, resulting in a −1 frameshift starting in the next exon (Fig. 1c). This hypothesis is supported by our minigene assay, although a mutant transcript with intron-1 retention was also observed. Similarly, a common AI-causing *ENAM* mutation (NM_031889.2:c.588+1del), which removes one G out of repeat sequence of seven Gs, at the Exon 9-Intron 9 junction has been suspected to cause a −1

frameshift rather than altered mRNA splicing.[22,26] For *ODAPH* TV1, this frameshift would cause the production of a mutant isoform 1 with a normal signal peptide but an aberrant secreted protein. Interestingly, for TV2, the odd combination of a natural and a pathological shift in reading frames makes the mutant isoform 2 equal to normal isoform 1 but lacking the exon 2 encoded 15 amino acid (ALST-FYLQQHINLHM) segment (Fig. 3). Therefore, while no functional ODAPH isoform 2 exists, a nearly intact isoform 1 is presumably produced in patients with this specific mutation. This finding suggests that ODAPH isoform 1 is probably not sufficient to compensate for loss of isoform 2 function and most likely plays little, if any, role in enamel formation. The fourth mutation is at the splice acceptor site of intron 2 and likely forces the skipping of exon 3 (the last coding exon) in TV1 and TV2. Presumably, these transcripts would be degraded by nonsense mediated decay. The last 3 mutations are all single nucleotide variants in exon 3 that introduce a premature termination codon (nonsense mutation) for TV2. However, due to a different reading frame, they would cause 2 missense mutations (p.Ala58Asp, p.Gly121Asp) and a synonymous variant (p.His91 =) respectively on TV1 products. Noticeably, the last 2 nonsense mutations for TV2 are located at the region of exon 3 deleted in TV3 by alternative splicing, indicating no impact on TV3 from the mutations (Fig. 3). The presence of intact TV3 in AI patients with these 2 specific mutations however suggests an insignificant role for ODAPH isoform 3 on enamel development. In summary, analyses of molecular consequences of 7 known *ODAPH* disease-causing mutations on different transcripts strongly suggest that isoform 2 might be the single dominant *ODAPH* transcript product critical for dental enamel formation. Moreover, there is only one *Odaph* transcript identified in mouse, which encodes only 2 exons and is analogous to human TV2.[11,21] The lack of other transcripts indicates the only isoform of mouse ODAPH protein is sufficient for normal amelogenesis, which further supports our hypothesis.

Although two mouse models of defective *Odaph* were recently reported to recapitulate failed enamel maturation in human AI,[27,28] the cellular and molecular functions of ODAPH remain largely unknown. It was demonstrated that *Odaph* is expressed by the ameloblasts at the onset of post-secretory transition in mouse mandibular incisors. ODAPH protein was detected at the basal lamina between enamel and maturation stage ameloblasts in mouse incisors and molars, suggesting a role in cell-matrix adhesion. No expression was detected in other dental tissues. However, in this study, we showed that dental pulp cells of human primary teeth express *ODAPH* TV2. Weak expression was also detected in dental follicles of developing teeth, presumably from cells of the reduced enamel epithelium, which also exhibited *KLK4* expression. Interestingly, expression of *AMTN*, a gene encoding a basal lamina protein during maturation stage of amelogenesis, is also observed in dental pulp tissues. These findings indicate species differences in *ODAPH* expression and suggest a role for ODAPH in the dentin-pulp complex, presumably in dentin formation. This hypothesis is supported by phylogenetic studies. It has been demonstrated that *ODAPH* is specifically inactivated in mammalian species that have lost the ability (during evolution) to make teeth but not in those with enamel-less teeth, indicating that *ODAPH* is functionally tooth-specific rather than enamel-specific.[21] However, no dentin phenotypes have been documented in families with *ODAPH* mutations.[11,25] In this study, we found no clinically detectable dentin defect in our patients. Further investigations are warranted to study the molecular pathogenesis of *ODAPH*-associated AI and to unravel the functions of ODAPH in enamel formation and potentially during dentin development.

In summary, our study demonstrates that loss-of-function *ODAPH* mutations can cause autosomal recessive hypocalcified amelogenesis imperfecta and argues that isoform 2 of ODAPH proteins is probably the only isoform critical for dental enamel formation. Furthermore, we show that *ODAPH* is expressed by dental pulp tissues and might play important roles in development and homeostasis of dentin-pulp complex.

Declaration of competing interest

The authors have no conflicts of interest relevant to this article.

Acknowledgments

Appendix A. Supplementary data

Supplementary data to this article can be found online at https://doi.org/10.1016/j.jds.2023.09.020.

References

1. Witkop CJ. Hereditary defects in enamel and dentin. *Acta Genet Stat Med* 1957;7:236—9.
2. Witkop CJ. Amelogenesis imperfecta, dentinogenesis imperfecta and dentin dysplasia revisited: problems in classification. *J Oral Pathol* 1988;17:547—53.
3. Smith CEL, Poulter JA, Antanaviciute A, et al. Amelogenesis imperfecta; genes, proteins, and pathways. *Front Physiol* 2017;8:435.
4. Lagerström M, Dahl N, Nakahori Y, et al. A deletion in the amelogenin gene (AMG) causes X-linked amelogenesis imperfecta (AIH1). *Genomics* 1991;10:971—5.
5. Rajpar MH, Harley K, Laing C, Davies RM, Dixon MJ. Mutation of the gene encoding the enamel-specific protein, enamelin, causes autosomal-dominant amelogenesis imperfecta. *Hum Mol Genet* 2001;10:1673—7.

6. Poulter JA, Murillo G, Brookes SJ, et al. Deletion of ameloblastin exon 6 is associated with amelogenesis imperfecta. *Hum Mol Genet* 2014;23:5317—24.
7. Kim JW, Simmer JP, Hart TC, et al. MMP-20 mutation in autosomal recessive pigmented hypomaturation amelogenesis imperfecta. *J Med Genet* 2005;42:271—5.
8. Hart PS, Hart TC, Michalec MD, et al. Mutation in kallikrein 4 causes autosomal recessive hypomaturation amelogenesis imperfecta. *J Med Genet* 2004;41:545—9.
9. Kim JW, Lee SK, Lee ZH, et al. FAM83H mutations in families with autosomal-dominant hypocalcified amelogenesis imperfecta. *Am J Hum Genet* 2008;82:489—94.
10. El-Sayed W, Parry DA, Shore RC, et al. Mutations in the beta propeller WDR72 cause autosomal-recessive hypomaturation amelogenesis imperfecta. *Am J Hum Genet* 2009;85:699—705.
11. Parry DA, Brookes SJ, Logan CV, et al. Mutations in C4orf26, encoding a peptide with in vitro hydroxyapatite crystal nucleation and growth activity, cause amelogenesis imperfecta. *Am J Hum Genet* 2012;91:565—71.
12. Parry DA, Poulter JA, Logan CV, et al. Identification of mutations in SLC24A4, encoding a potassium-dependent sodium/calcium exchanger, as a cause of amelogenesis imperfecta. *Am J Hum Genet* 2013;92:307—12.
13. Poulter JA, Brookes SJ, Shore RC, et al. A missense mutation in ITGB6 causes pitted hypomineralized amelogenesis imperfecta. *Hum Mol Genet* 2014;23:2189—97.
14. Wang SK, Choi M, Richardson AS, et al. ITGB6 loss-of-function mutations cause autosomal recessive amelogenesis imperfecta. *Hum Mol Genet* 2014;23:2157—63.
15. Parry DA, Smith CE, El-Sayed W, et al. Mutations in the pH-sensing G-protein-coupled receptor GPR68 cause amelogenesis imperfecta. *Am J Hum Genet* 2016;99:984—90.
16. Seymen F, Kim YJ, Lee YJ, et al. Recessive mutations in ACPT, encoding testicular acid phosphatase, cause hypoplastic amelogenesis imperfecta. *Am J Hum Genet* 2016;99:1199—205.
17. Kim JW, Zhang H, Seymen F, et al. Mutations in RELT cause autosomal recessive amelogenesis imperfecta. *Clin Genet* 2019;95:375—83.
18. Dong J, Amor D, Aldred MJ, Gu T, Escamilla M, MacDougall M. DLX3 mutation associated with autosomal dominant amelogenesis imperfecta with taurodontism. *Am J Med Genet* 2005;133A:138—41.
19. Kim JW, Seymen F, Lee KE, et al. LAMB3 mutations causing autosomal-dominant amelogenesis imperfecta. *J Dent Res* 2013;92:899—904.
20. Poulter JA, El-Sayed W, Shore RC, Kirkham J, Inglehearn CF, Mighell AJ. Whole-exome sequencing, without prior linkage, identifies a mutation in LAMB3 as a cause of dominant hypoplastic amelogenesis imperfecta. *Eur J Hum Genet* 2014;22:132—5.
21. Springer MS, Starrett J, Morin PA, Lanzetti A, Hayashi C, Gatesy J. Inactivation of C4orf26 in toothless placental mammals. *Mol Phylogenet Evol* 2016;95:34—45.
22. Zhang H, Hu Y, Seymen F, et al. ENAM mutations and digenic inheritance. *Mol Genet Genomic Med* 2019;7:e00928.
23. Vis JK, Vermaat M, Taschner PE, Kok JN, Laros JF. An efficient algorithm for the extraction of HGVS variant descriptions from sequences. *Bioinformatics* 2015;31:3751—7.
24. Adzhubei IA, Schmidt S, Peshkin L, et al. A method and server for predicting damaging missense mutations. *Nat Methods* 2010;7:248—9.
25. Prasad MK, Laouina S, El Alloussi M, Dollfus H, Bloch-Zupan A. Amelogenesis imperfecta: 1 family, 2 phenotypes, and 2 mutated genes. *J Dent Res* 2016;95:1457—63.
26. Kida M, Ariga T, Shirakawa T, Oguchi H, Sakiyama Y. Autosomal-dominant hypoplastic form of amelogenesis imperfecta caused by an enamelin gene mutation at the exon-intron boundary. *J Dent Res* 2002;81:738—42.
27. Ji Y, Li C, Tian Y, et al. Maturation stage enamel defects in odontogenesis-associated phosphoprotein (Odaph) deficient mice. *Dev Dynam* 2021;250:1505—17.
28. Liang T, Hu Y, Kawasaki K, et al. Odontogenesis-associated phosphoprotein truncation blocks ameloblast transition into maturation in Odaph(C41∗/C41∗) mice. *Sci Rep* 2021;11:1132.